Physics Letters B 717 (2012) 371–375

Contents lists available at SciVerse ScienceDirect

Physics Letters B

www.elsevier.com/locate/physletb

Discovery and cross-section measurement of neutron-rich isotopes in the element range from neodymium to platinum with the FRS

J. Kurcewicz [a,*], F. Farinon [a,b,1], H. Geissel [a,b], S. Pietri [a], C. Nociforo [a], A. Prochazka [a,b], H. Weick [a], J.S. Winfield [a], A. Estradé [a,c], P.R.P. Allegro [d], A. Bail [e], G. Bélier [e], J. Benlliure [f], G. Benzoni [g], M. Bunce [h], M. Bowry [h], R. Caballero-Folch [i], I. Dillmann [a,b], A. Evdokimov [a,b], J. Gerl [a], A. Gottardo [j], E. Gregor [a], R. Janik [k], A. Kelić-Heil [a], R. Knöbel [a], T. Kubo [l], Yu.A. Litvinov [a,m], E. Merchan [a,n], I. Mukha [a], F. Naqvi [a,o], M. Pfützner [a,p], M. Pomorski [p], Zs. Podolyák [h], P.H. Regan [h], B. Riese [a,b], M.V. Ricciardi [a], C. Scheidenberger [a,b], B. Sitar [k], P. Spiller [a], J. Stadlmann [a], P. Strmen [k], B. Sun [b,q], I. Szarka [k], J. Taïeb [e], S. Terashima [a,l], J.J. Valiente-Dobón [j], M. Winkler [a], Ph. Woods [r]

[a] GSI Helmholtzzentrum für Schwerionenforschung, 64291 Darmstadt, Germany
[b] Justus-Liebig-Universität Gießen, 35392 Gießen, Germany
[c] Astronomy and Physics Department, Saint Mary's University, Halifax, Nova Scotia B3H 3C3, Canada
[d] Institute of Physics, Universidade de São Paulo, CEP 05508-090 Cidade Universitária, São Paulo, Brazil
[e] CEA DAM DiF, 91290 Arpajon Cedex, France
[f] Universidad de Santiago de Compostela, E-15706 Santiago de Compostella, Spain
[g] INFN sezione di Milano, I-20133 Milano, Italy
[h] Department of Physics, University of Surrey, Guildford, Surrey, GU2 7XH, UK
[i] Universitat Politècnica de Catalunya, 08034 Barcelona, Spain
[j] INFN – Laboratori Nazionali di Legnaro, 35020 Legnaro, Italy
[k] Faculty of Mathematics and Physics, Comenius University, 842 48 Bratislava, Slovakia
[l] RIKEN Nishina Center, RIKEN, Wako, Saitama 351-0198, Japan
[m] Max-Planck-Institut für Kernphysik, 69117 Heidelberg, Germany
[n] Institut für Kernphysik, Technische Universität Darmstadt, 62289 Darmstadt, Germany
[o] Institut für Kernphysik, Universität zu Köln, 50937 Köln, Germany
[p] Faculty of Physics, University of Warsaw, 00-681 Warsaw, Poland
[q] School of Physics and Nuclear Energy Engineering, Beihang University, Beijing 100191, China
[r] School of Physics, University of Edinburgh, Edinburgh, EH9 3JZ, UK

ARTICLE INFO

Article history:
Received 1 December 2011
Received in revised form 26 July 2012
Accepted 10 September 2012
Available online 12 September 2012
Editor: D.F. Geesaman

ABSTRACT

Using the high-resolution performance of the fragment separator FRS at GSI we have discovered 60 new neutron-rich isotopes in the atomic number range of $60 \leqslant Z \leqslant 78$. The new isotopes were unambiguously identified in reactions with a ^{238}U beam impinging on a Be target at 1 GeV/nucleon. The production cross-section for the new isotopes have been measured down to the pico-barn level and compared with predictions of different model calculations. For elements above hafnium fragmentation is the dominant reaction mechanism which creates the new isotopes, whereas fission plays a dominant role for the production of the new isotopes up to thulium.

1. Introduction

Heavy neutron-rich nuclides are of great interest for nuclear astrophysics and basic nuclear spectroscopy. This becomes immediately obvious when one looks at the predicted path for r-process nuclei and their decay. The study of shell evolution far off stability and towards the expected magic numbers $N = 82$, 126 and thus the waiting points of the r-process nuclides are of interest for both fields. The accurate knowledge of the atomic masses and lifetimes are essential for the understanding of the nucleosynthesis [1–3]. Presently, the corresponding theories, when applied to newly opened experimental territories, still deviate significantly from the results of measurements.

Experimentally the area of heavy neutron-rich nuclides is difficult to reach because of the low production cross-sections and the great challenge of separation and isotopic identification. Relativistic energies of the reaction products and the high ion-optical

* Corresponding author.
E-mail address: j.kurcewicz@gsi.de (J. Kurcewicz).
[1] Part of PhD work, Justus-Liebig University, Gießen, 2011.

0370-2693
http://dx.doi.org/10.1016/j.physletb.2012.09.021

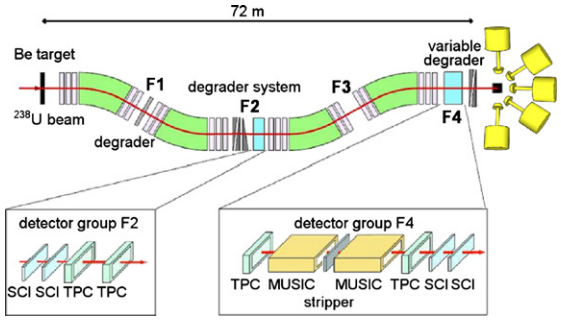

Fig. 1. (Color online.) Schematic view of the four magnetic dipole stages of the FRS with the target area and the detector and degrader systems at the focal planes.

resolution of the in-flight separator FRS [4] are the keys to the frontiers in this domain of nuclides. High velocities are required to reduce the number of populated ionic charge-states for each element, mainly to bare fragments with a low contamination of H- and He-like ions.

In recent years, the intensity of ^{238}U beams provided by the GSI accelerators has increased almost by a factor of 10, which has opened new opportunities for the production and study of the heaviest projectile fragments [5,6]. Along with mass measurements at the FRS–ESR facility several new isotopes have been observed [6,7]. Taking advantage of the improved experimental conditions we aimed at the production of very neutron-rich nuclides with a 1 GeV/nucleon ^{238}U beam. In this Letter we report the main results of this study: the discovery of 60 new neutron-rich isotopes in the element range from $_{60}$Nd to $_{78}$Pt and the determination of their production cross-sections.

2. Experimental technique

The experiment was performed with the SIS-18 synchrotron of GSI Darmstadt, which delivered a 1 GeV/nucleon ^{238}U beam in spills lasting 0.5–2 s with a repetition period of 2–4 s. The beam impinged on a 1.6 g/cm^2 thick beryllium target placed at the entrance of the projectile Fragment Separator (FRS) [4]. The primary beam intensity was of the order of 2×10^9 ions/spill. The ^{238}U intensity was measured by a calibrated secondary-electron transmission monitor [8]. The reaction products were separated by the FRS operated in an overall achromatic ion-optical mode. A schematic view of the FRS and the experimental setup is shown in Fig. 1. The spatial separation in flight was achieved by a twofold application of the $B\rho$–ΔE–$B\rho$ method, i.e., the atomic energy losses in two degraders, located at the first (F1) and second (F2) focal planes, were measured via magnetic rigidity analysis. In this way, the reaction products are spatially separated and by the use of various detectors their nuclear charge Z and mass number A could be determined. After the first magnetic selection and the 2.5 g/cm^2 thick aluminum degrader at F1, the reaction products were slowed down in an aluminum wedge degrader located at the intermediate focal plane F2. By changing the wedge angle, the degrader shape was tuned to preserve the achromatism. Even at these relativistic velocities different atomic charge states of the heavy fragments have to be considered. Therefore, a niobium foil was placed behind the target to enhance the population of bare fragments. The thin titanium vacuum window of the F2 section acts in the same way. The thicknesses of these electron strippers were 223 mg/cm^2 (Nb) for the first and 90 mg/cm^2 (Ti) for the latter. The total thickness of the F2-matter including detectors was 1.32 g/cm^2 aluminum equivalent. After penetrating the F2-matter the heaviest fragments emerged as 81% fully ionized, 18.5% H-like and 0.5% He-like ions.

The complete particle identification in-flight was performed on an event-by-event basis with time-of-flight (ToF), energy-deposition ($\Delta E'$) and magnetic rigidity measurements (ToF–$\Delta E'$–$B\rho$ method). The ToF was measured with two plastic scintillator detectors (SCI), one located at F2 and the other at the final focal plane (F4). The time resolution was about 30 ps (standard deviation). The ToF value for the selected isotopes was of the order of 160 ns in the laboratory frame. A second pair of ToF detectors was used in the experiment providing a redundant time measurement. At the exit of the FRS, two ionization chambers (MUSIC) filled with P10 gas at atmospheric pressure were mounted with a 104 mg/cm^2 copper stripper placed in between. The MUSIC detectors [9,10] delivered the energy-deposition signals of fragments, thus providing the information of their atomic numbers. The velocity dependence of the penetrating ions was taken into account before the encoded energy-deposition information was used for Z identification. The obtained Z resolution was better than 1%. The magnetic rigidity was measured with four time-projection chambers (TPC) [11], two located at the dispersive focal plane (F2) and the other two mounted at the exit of the FRS. The TPC provided full tracking information (angle and position) for the transmitted fragments. The $B\rho$ resolution, deduced from the position measurements, was better than 10^{-4}. Furthermore, the four TPC detectors also provided energy-deposition information, an additional condition in our analysis, which contributes to reduce further background signals in the region of low statistics for the most neutron-rich isotopes. The event-by-event identification, and thus also the in-flight separation, were verified by the isomer tagging technique [12]. In the particle identification spectrum, known μs isomers were selected (^{171m}Tm, ^{172m}Yb and ^{175m}Lu) whose gamma rays were recorded in coincidence with the incoming ions stopped in a layer of matter viewed either by the RISING germanium detector setup [13], or the simpler isomer tagging device [12], which consisted of only two Ge detectors, a stopper foil, and a veto scintillator. With these manifold redundant measurements and the two-stage in-flight separation criteria, we achieved an unambiguous isotope identification.

3. Data analysis

In the experiment the $B\rho$ was set to four different values: (11.799 Tm), (10.796 Tm), (11.091 Tm), and (11.368 Tm), which were chosen to yield optimum intensities for bare ^{172}Dy, ^{194}Os, ^{198}Os, and ^{202}Os ions, respectively. The data collected for each field setting were processed by the following procedure based on a combination of ToF, position and energy-deposition information.

In the first step of the analysis a two-dimensional plot of the energy-deposition in the first MUSIC detector as a function of the energy-deposition in the second MUSIC detector was created. We set a condition on the events corresponding to the full energy deposition in both detectors to select a well-defined atomic number Z. In the second step, a distribution of Z as a function of the difference of the $B\rho$ values between the second and the third sections of the FRS was analyzed. This difference reflects the energy loss of ions in the matter placed at the intermediate focal plane F2, which was calculated from the position measurements at the intermediate and the final focal planes. In this step a selection is made to strongly suppress events which correspond to ions which changed their charge while passing through the materials at the F2 focal plane. Finally, using the events selected in the two previous steps, a correlation of the position in the final focal plane F4 with the mass-over-charge ratio, A/q, is plotted for the selected atomic number Z. By use of the programs MOCADI [14] and LISE++ [15] we have verified that only the nuclei which were transmitted through the whole FRS as fully stripped ions appear in the cen-

Table 1
Production cross-sections for the new isotopes measured in the present work. The isotopes marked with a * were already claimed [30–33] but they are not listed in the evaluation work of Thoennessen et al. [34].

Isotope	σ (nb)	Isotope	σ (nb)	Isotope	σ (nb)	Isotope	σ (nb)
^{157}Nd*	980(40)	^{168}Gd	78(5)	^{176}Er	68(5)	^{188}Lu	0.010(3)
^{158}Nd*	201(11)	^{169}Gd	10.6(15)	^{177}Er	18(2)	^{190}Hf*	0.027(13)
^{159}Nd	39(4)	^{170}Gd	2.6(8)	^{178}Er	5.5(9)	^{193}Ta	0.017(5)
^{160}Nd	9.5(22)	^{169}Tb	751(28)	^{178}Tm*	24(3)	^{194}Ta	0.0037(19)
^{161}Nd	3.0(17)	^{170}Tb	99(6)	^{179}Tm	1.21(18)	^{195}W*	0.049(1)
^{160}Pm	518(36)	^{171}Tb	14(2)	^{180}Tm	4.5(9)	^{196}W	0.018(4)
^{161}Pm	161(9)	^{172}Tb	1.0(4)	^{181}Tm	0.6(3)	^{197}W	0.0034(17)
^{162}Pm	25(3)	^{171}Dy	441(18)	^{181}Yb*	2.3(3)	^{198}Re*	0.028(7)
^{163}Pm	4.5(15)	^{172}Dy	121(7)	^{182}Yb*	0.45(10)	^{199}Re	0.0076(27)
^{163}Sm	134(11)	^{173}Dy	18(2)	^{183}Yb	0.21(5)	^{202}Os	0.0044(20)
^{164}Sm	42(4)	^{174}Dy	1.9(6)	^{184}Yb	0.028(9)	^{203}Os	0.0025(18)
^{165}Sm	7.8(16)	^{173}Ho	341(15)	^{185}Yb	0.007(3)	^{205}Ir	0.003(2)
^{167}Eu	7.1(12)	^{174}Ho	98(6)	^{185}Lu*	0.22(7)	^{206}Pt	0.033(11)
^{168}Eu	2.0(8)	^{175}Ho	22(2)	^{186}Lu*	0.15(4)	^{207}Pt	0.008(3)
^{167}Gd	625(23)	^{176}Ho	2.2(6)	^{187}Lu	0.043(9)	^{208}Pt	0.0027(15)

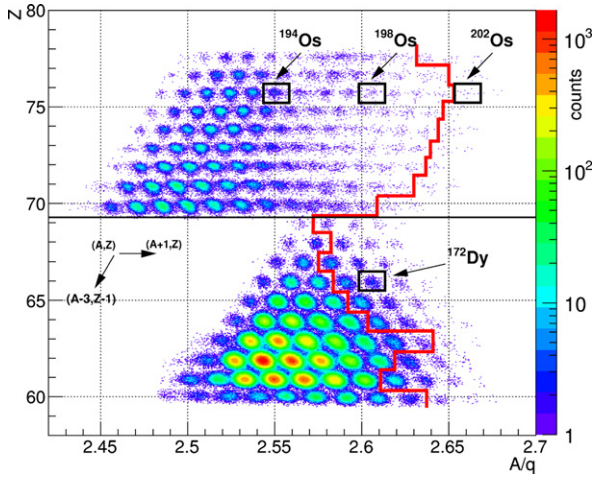

Fig. 2. (Color online.) Identified atomic number Z of the incoming ions as a function of their A/q ratio at the final focal plane (F4). In the A/q ratio, the time-of-flight and magnetic rigidity information is included. The plot shows the superimposed data recorded in the different $B\rho$ settings for bare ^{194}Os, ^{198}Os, ^{202}Os ions separated by the horizontal line from the ^{172}Dy field setting. Events corresponding to these ions are marked by open rectangles. The discovered new isotopes are on the right hand side of the staggered solid line.

tral position at the final focus. Thus, a gate imposed on this plot rejected the remaining impurities, like particles which passed the central focal plane F2 as H-like ions and also those which picked-up or lost one electron at F2 but were not rejected in the second step. By applying this procedure to all isotopic chains, the final identification spectrum of atomic number Z versus A/q can be created. The superposition of such spectra corresponding to all settings of the FRS is shown in Fig. 2.

Since the charge-changing events within the MUSIC detectors limit the Z determination for the heaviest ions, the selected events for a given Z may have a small contamination from neighboring elements. The simulations indicate [15,14] that in such cases, the isotope selected by our procedure, characterized by (A, Z), may contain a small contamination from nuclei with numbers $A-5$ and $Z-1$ which are transmitted through the FRS as H-like ions. Both the selected isotope and the contaminants will have almost identical magnetic rigidity and position distributions. To estimate the level of such a contamination, we note that in the investigated region the production cross-sections for a contaminant is larger by up to a factor of 50 compared with the cross-sections of the isotopes of interest (see data in Table 1). However, the probability that an ion passes through the whole FRS in the H-like state is of the order of 10^{-4}. We can conclude that isotopes selected by our identification procedure have a negligible contamination, at the level of 5×10^{-3}.

4. Production cross-sections

The data recorded for each $B\rho$ setting were analyzed by the procedure described above to achieve a reliable isotope identification. In the next step the production cross-sections of individual isotopes were determined according to:

$$\sigma_f = \frac{N_f}{N_p N_t \epsilon}, \tag{1}$$

where N_f is the number of recorded ions for a selected isotope, N_p the total number of ^{238}U ions, N_t the number of target atoms and ϵ takes into account the ion-optical transmission, the secondary reactions in the matter placed after the target (e.g., degraders and detectors), the probability that an ion remains fully stripped in both stages of the separator, the absorption from secondary nuclear reactions in the target and the dead-time losses of the data acquisition system. All secondary reactions in the target and the matter in the focal planes are taken into account by applying the Benesh–Cook–Vary formula [16].

The code GLOBAL [17] provided the charge-state population for the fragments during their passage through the FRS system. The probability values for bare Nd to Pt ions ranged from 0.9 to 0.6, respectively. The ion-optical transmissions have been calculated by the Monte-Carlo simulation program MOCADI [14] taking into account the different kinematics of projectile fragmentation and fission [18,14]. The contribution of each reaction type was calculated for the observed nuclides using the ABRABLA program [19,20]. The corresponding weighted transmission coefficient was used in the cross section calculation. The transmission values were obtained separately for each $B\rho$ setting. The typical values for projectile fragments were of the order of 0.4–0.6 for isotopes with A/q close to the reference setting. This relatively small value is due to the tight slits settings in the FRS, which were applied in order to decrease the number of contaminants reaching the F4 area, mainly fragments with $Z < 60$ coming from low-energy fission.

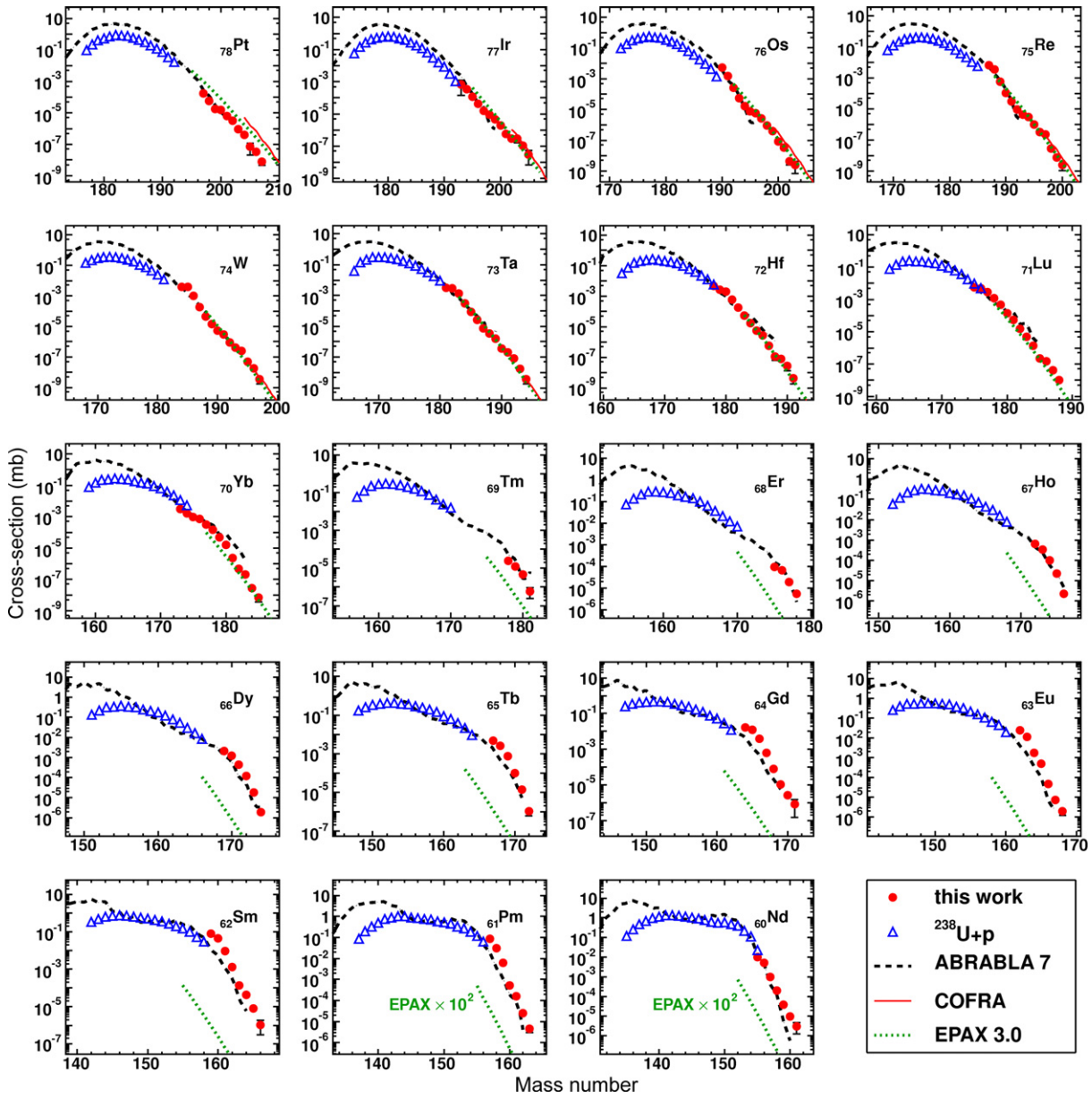

Fig. 3. (Color online.) Measured production cross-sections of fragments produced in the reaction ^{238}U (1 GeV/nucleon) + Be (red circles), shown together with the results of Refs. [21–23] which used the reaction ^{238}U (1 GeV/nucleon) + p (blue open triangles). The back dashed line represents the predictions of the ABRABLA model [19,20] and the continuous red line shows the results of COFRA [24] ($Z = 73$–78). The green dotted line shows the prediction of EPAX-3 model [25]. All three calculations were done for the reaction 1 GeV/nucleon ^{238}U + Be. The predictions of EPAX-3 for the elements $_{60}$Nd and $_{61}$Pm are multiplied by a factor of 100 to keep the range of axes constant.

5. Results

The measured heavy neutron-rich isotopes, in the atomic numbers range of $60 \leqslant Z \leqslant 78$, and their production cross sections are plotted in Fig. 3 and listed in Table 1. For all isotopes discovered in this work we can state that the lifetime must be long enough to survive the 300 ns time of flight between the production target and final focal plane.

The isotopic production cross-section have been determined in this experiment down to the pico-barn level. In particular, the steep descent of the yields of the neutron-rich isotopes has been mapped. The error bars are determined by the statistics and the systematical uncertainties in the calculations of the transmission.

The cross-sections measured in this experiment are compared with experimental results of less exotic nuclides [21–23] in Fig. 3. Although the latter data from the literature are obtained from reactions of 1 GeV/nucleon ^{238}U beam with a liquid hydrogen target, the continuous transition of the two experimental data sets is remarkable. The excitation in the reaction with hydrogen target nuclei should be in the average lower than in our case with a beryllium target but this plays apparently a minor role for the compared fragment distribution in the overlap region.

Fig. 3 shows also the predictions of three different of model calculations: ABRABLA [19,20], COFRA [24] and EPAX-3 [25]. The ABRABLA is a two-stage abrasion–ablation model. The excited prefragments formed in the first stage of reaction (abrasion) [19], deexcite in the second stage (ablation) via emission of photons, particles (neutrons, ^{1,2,3}H, ^{3,4}He), intermediate-mass-fragments and by fission [20]. The ABRABLA model has shown in the past a good predictive power which is documented in Refs. [26–29] especially due to the elaborated description of fission. The COFRA code is based on a simplified version of the abrasion–ablation model where

the only considered decay channel is neutron evaporation. This assumption allows an analytical description of the ablation process, thus, reducing considerably the calculation time for the most neutron-rich nuclei. Due to this assumption, the validity domain of the COFRA program is limited to residual nuclei with large neutron excess, which are not produced via fission. EPAX-3 is based on a semi-empirical parametrization for production cross-sections of fragmentation–evaporation and does not explicitly include the contribution of fission. The effect of this limitation is clearly visible in Fig. 3. Note that all calculations presented here have been performed for the reaction 1 GeV/nucleon ^{238}U + Be and should not be directly compared with the experimental results from Refs. [21–23] which have been obtained for ^{1}H target.

The ABRABLA predictions show an overall good agreement with the experimental data measured in the present work. Based on the results of ABRABLA calculations we can say that the observed new neutron-rich isotopes of the elements between $60 \leqslant Z \leqslant 69$ are produced dominantly by fission, while fragmentation plays a dominant role in the production of the isotopes of the elements above $Z = 72$. In the intermediate Z region both mechanisms contribute and a corresponding weighting factor was always applied for the correction of the transmission. Since ABRABLA is a Monte-Carlo program, it is difficult to calculate with enough statistics all production cross-sections over ten orders of magnitude. However, computer farming allowed us to calculate the production reactions for a significant part of our experimental data. For the most neutron-rich nuclei, predictions of the analytical COFRA code have been used for the range of elements where fragmentation is dominant. The COFRA model is in general also in good agreement with the experimental data, although gradual deviations from the experimental results can be observed for the heaviest (Os–Pt) nuclei. It should be stressed that the predictions of COFRA are extremely sensitive to the precise values of the neutron separation energies of the nuclei of interest which are not well or not known at all for all nuclei measured in the present work. For most of the fragmentation cases in Fig. 3, there is an overestimation by COFRA by no more than a factor of two compared with the measured values. This means COFRA may be well suited to make valid predictions for new studies in the field of heavy neutron-rich isotopes. The EPAX-3 predictions are also quite good in the region of neutron-rich nuclei where fragmentation dominates. For the neutron-rich low-Z nuclides EPAX-3 cannot reliably predict the cross-sections because fission is not included in the parametrization.

6. Summary

In the range of heavy neutron-rich nuclides the results of the present experiment opens up a new field for nuclear structure and reaction studies and also for nuclear astrophysics. With the redundant detector setup and the high-resolution performance of the fragment separator FRS we discovered 60 new isotopes in the range of atomic numbers of $60 \leqslant Z \leqslant 78$. The new isotopes have been unambiguously identified in the reaction of 1 GeV/nucleon ^{238}U projectiles with a beryllium target. The isotopic production cross-section for the most neutron-rich isotopes have been measured and compared with the predictions of the ABRABLA, COFRA, and EPAX-3 models. All models give an overall good agreement, within their limits of validity, with the data measured in the present experiment. This observation makes them potentially useful for future predictions of production yields of nuclei in unknown territories. The next steps in this experimental campaign will be half-life and mass measurements, as well as decay spectroscopy after implantation in silicon detectors.

Acknowledgements

It is a pleasure to thank the technical staff of the accelerators, the FRS, and the target laboratory for their valuable contribution to the beam quality and experimental setups. The authors gratefully acknowledge fruitful discussions with G. Martinez-Pinedo, K. Otsuki and B. Pfeiffer. We would like to thank M. Thoennessen for his contributions with respect to the isotope-evaluation literature. This work was supported by STFC (UK). B. Sun is partially supported by NECT and NSFC 11105010.

References

[1] F. Käppeler, F.K. Thielemann, M. Wiescher, Ann. Rev. Part. Nucl. Science 48 (1998) 175.
[2] B. Franzke, H. Geissel, G. Münzenberg, Mass Spectrom. Rev. 27 (5) (2008) 428.
[3] I.U. Roederer, et al., Astrophys. J. 698 (2009) 1963.
[4] H. Geissel, et al., Nucl. Instrum. Methods Phys. Res. B 70 (1992) 286.
[5] H. Alvarez-Pol, et al., Phys. Rev. C 82 (2010) 041602(R).
[6] L. Chen, et al., Phys. Lett. B 691 (2010) 234.
[7] H. Geissel, et al., Eur. Phys. J. Spec. Top. 150 (2007) 109.
[8] B. Jurado, K.-H. Schmidt, K.-H. Behr, Nucl. Instrum. Methods Phys. Res. A 483 (2002) 603.
[9] M. Pfützner, et al., Nucl. Instrum. Methods Phys. Res. B 86 (1994) 213.
[10] A. Stolz, et al., GSI Scientific Report, 1998, p. 174.
[11] R. Janik, et al., Nucl. Instrum. Methods Phys. Res. A 640 (2011) 54.
[12] F. Farinon, PhD thesis, Justus Liebig University Giessen, 2011.
[13] S. Pietri, et al., Nucl. Instrum. Methods Phys. Res. B 261 (2007) 1079.
[14] N. Iwasa, et al., Nucl. Instrum. Methods Phys. Res. B 126 (1997) 284.
[15] O. Tarasov, D. Bazin, Nucl. Instrum. Methods Phys. Res. B 266 (2008) 4657.
[16] C. Benesh, B. Cook, J. Vary, Phys. Rev. C 40 (1989) 1198.
[17] C. Scheidenberger, et al., Nucl. Instrum. Methods Phys. Res. B 142 (1998) 441.
[18] D.J. Morrissey, Phys. Rev. C 39 (1989) 460.
[19] J.-J. Gaimard, K.-H. Schmidt, Nucl. Phys. A 531 (1991) 709.
[20] A. Kelić, M.V. Ricciardi, K.-H. Schmidt, in: Proceedings of the Joint ICTP-IAEA Advanced Workshop on Model Codes for Spallation Reactions, 4–8 February 2008, ICTP Trieste, Italy, IAEA INDC(NDS)-530, 2008, pp. 181–221.
[21] M. Bernas, et al., Nucl. Phys. A 725 (2003) 213.
[22] M. Bernas, et al., Nucl. Phys. A 765 (2006) 197.
[23] J. Taieb, et al., Nucl. Phys. A 724 (2003) 413.
[24] J. Benlliure, et al., Nucl. Phys. A 660 (1999) 87.
[25] K. Sümmerer, Phys. Rev. C 86 (2012) 014601, http://www.gsi.de/documents/FRS-reference-2012-001.html.
[26] M.V. Ricciardi, et al., Phys. Rev. C 73 (2006) 014607.
[27] J. Kurcewicz, et al., Nucl. Phys. A 767 (2006) 1.
[28] J.C. David, et al., CEA Saclay internal report DAPNIA-07-59 for EURISOL-DS Task 11, 2007.
[29] A. Boudard, et al., Phys. Rev. C 66 (2002) 044615.
[30] M. Bernas, et al., Nucl. Phys. A 616 (1997) 352c.
[31] Zs. Podolyak, et al., in: Proc. 2nd Intern. Conf. Fission and Properties of Neutron-Rich Nuclei, St Andrews, Scotland, June 28–July 3, 1999, World Scientific, Singapore, 2000, p. 156.
[32] S.D. Al-Garni, et al., GSI Scientific Report, 2001, p. 13.
[33] T. Kurtukian-Nieto, et al., J Phys. Conf. Series 202 (2010) 012012.
[34] M. Thoennessen, et al., http://www.nscl.msu.edu/~thoennes/isotopes/.